Acta Crystallographica Section D
Biological Crystallography
ISSN 0907-4449

Structure of recombinant human cyclophilin J, a novel member of the cyclophilin family

Li-Li Huang,[a]‡ Xue-Mei Zhao,[b]‡ Chao-Qun Huang,[b] Long Yu[b]* and Zong-Xiang Xia[a]*

[a]State Key Laboratory of Bio-organic and Natural Products Chemistry, Shanghai Institute of Organic Chemistry, Chinese Academy of Sciences, Shanghai 200032, People's Republic of China, and [b]State Key Laboratory of Genetic Engineering of China, Institute of Genetics, School of Life Science, Fudan University, Shanghai 200433, People's Republic of China

‡ These authors made equal contributions to this work.

Correspondence e-mail: longyu@fudan.edu.cn, xiazx@mail.sioc.ac.cn

Received 4 October 2004
Accepted 15 December 2004

PDB Reference: cyclophilin J, 1xyh, r1xyhsf.

Cyclophilins (CyPs) are a large class of highly conserved ubiquitous peptidyl-prolyl *cis–trans* isomerases. CyPs have also been identified as being a specific receptor for the immunosuppressive drug cyclosporin A and are involved in a variety of biological functions. CyPJ is a novel member of the CyP family and human CyPJ (hCyPJ) is the protein encoded by a cyclophilin-like gene from human foetal brain, which shows 50% sequence identity to human cyclophilin A (hCyPA). Recombinant hCyPJ was expressed in *Escherichia coli* and purified. The three-dimensional structure of hCyPJ has been determined by molecular replacement using the hCyPA structure as the search model and has been refined at 2.6 Å resolution. The hCyPJ molecule contains four helices and one β-barrel composed of eight antiparallel β-strands. The overall secondary and tertiary structures of hCyPJ are similar to those of hCyPA, but hCyPJ contains an additional disulfide bridge and four segments with conformations that are strikingly different from those of hCyPA. His43 and Gln52 of hCyPJ are expected to be the active sites based on sequence alignment with hCyPA. The hCyPJ structure shows a conserved water molecule close to His43 and Gln52 which appears to support the solvent-assisted mechanism.

1. Introduction

Cyclophilins (CyPs), FK506-binding protein and parvulins constitute a large class of peptidyl-prolyl *cis–trans* isomerases (PPIases; EC 5.2.1.8; Goethel & Marahiel, 1999; Karmela, 1995). Although the three classes of proteins are unrelated in primary sequences and dissimilar in structure, they all show PPIase activity, catalyzing the *cis–trans* isomerization of proline imidic peptide bonds in oligopeptide and protein substrates, which accelerates protein folding during protein synthesis in the cell. CyPs have also been identified as being specific receptors for the immunosuppressive drug cyclosporin A (CsA) and are involved in a variety of biological functions such as signal transduction and cell-cycle regulation. Recently, a human CyP was reported to bind to a protein of the human immunodeficiency virus 1 (HIV-1) virion and was found to be essential for infection with HIV to occur.

The CyPs are widely distributed in a variety of species from bacteria to mammals. The first discovered member of the CyP family was cyclophilin A (CyPA) from bovine thymocytes, which was identified to be a PPIase (Handschumacher *et al.*, 1984; Takahashi *et al.*, 1989). The three-dimensional structures of the unligated recombinant human T-cell cyclophilin A (hCyPA) and its complex with CsA and with a tetrapeptide and several dipeptides have been reported (Ke *et al.*, 1991; Ke, 1992; Mikol *et al.*, 1993; Kallen *et al.*, 1991; Ke, Mayrose *et al.*,

1993; Zhao & Ke, 1996). The structures of CyPA complexed with HIV-related proteins have also been reported (Gamble *et al.*, 1996; Zhao *et al.*, 1997). Other members of CyP family share sequence homology and exhibit three-dimensional structure similarity with CyPA (Ke, Zhao *et al.*, 1993; Mikol *et al.*, 1994; Reidt *et al.*, 2003).

Several different mechanisms have been proposed for the *cis–trans* interconversion of the peptidyl-prolyl bond catalyzed by CyPs (Zhao & Ke, 1996). However, each of them only explains part of the experimental data and the catalytic mechanism still remains controversial (Peterson *et al.*, 2000; Howard *et al.*, 2003). Therefore, further structure data of the CyP family will be helpful in understanding the functions and mechanism of CyPs.

CyPJ is a novel member of the CyP family. During a large-scale sequencing of a human foetal brain cDNA library, Zhou and coworkers isolated two cDNA clones which are different splicing variants of a novel cyclophilin-like gene PPIL3 (Zhou *et al.*, 2001). hCyPJ is the protein encoded by one of the two clones, PPIL3b, and shows 72% sequence identity to the cyclophilin isoform 10 of *Caenorhabditis elegans*. In this paper, we present the plasmid construction, protein expression, purification and the X-ray structure of hCyPJ.

2. Materials and methods

2.1. Plasmid construction

The 'in-frame' 0.5 kbp fragment of the hCyPJ gene was amplified from cDNA by polymerase chain reaction (PCR) with primers CEA (5′-ATA AGA AT**G CGG CCG C**TC TGT GAC ACT GCA TAA-3′) and CEB (5′-ATC G**CT CGA G**CT GAG CAA ATG GGT TGG CAT-3′). The two PCR primers contain *Not*I and *Xho*I restriction sites (in bold), respectively, to allow subcloning into the multiple cloning sites of the pTXB1 vector (NewEngland Biolab). The PCR products were sequentially digested with *Not*I and *Xho*I, gel-purified and ligated into the similarly digested vector pTXB1. The insert was confirmed by sequencing. Transformation of *Escherichia coli* ER2566 (NewEngland Biolabs) was carried out using the standard method.

2.2. Expression and purification

Recombinant hCyPJ was expressed following a 20 h induction with 0.2 m*M* IPTG at 295 K. The expressed protein was purified using a chitin-bead system, following the protocol provided by the manufacturer. Briefly, crude extract from *E. coli* containing fusion protein was passed over a 1 ml column at 277 K. The column was washed with more than ten column volumes of washing buffer (20 m*M* HEPES pH 8.0, 500 m*M* NaCl, 0.1 m*M* EDTA, 0.1% Triton X-100) and then quickly flushed with three column volumes of cleavage buffer (20 m*M* HEPES pH 8.0, 50 m*M* NaCl, 0.1 m*M* EDTA, 30 m*M* freshly diluted DTT). The column was then left at 277 K overnight. The hCyPJ protein was eluted with three column volumes of cleavage buffer without DTT. The purified protein was dialyzed three times with Millipore 10 000 against NH_4HCO_3. The dialyzed hCyPJ protein was frozen at 203 K overnight and then lyophilized for about 2 d. The hCyPJ protein powder was stored at 277 K.

Table 1
Crystal data and statistics of data collection and crystallographic refinement.

Data-collection statistics are for data set 2; statistics for data set 1 are not shown. Values in parentheses are for data in the highest resolution shell (2.69–2.60 Å).

Space group	$P3_121$
Unit-cell parameters (Å)	
a, *b*	41.3
c	172.1
No. of molecules per asymmetric unit	1
Matthews coefficient† ($Å^3$ Da^{-1})	2.35
Resolution (Å)	2.6
No. of unique reflections	5560
No. of observations	33855
Data completeness (%)	95.9 (92.4)
R_{merge}‡ (%)	8.4 (37.2)
Reflections with $I > 3\sigma(I)$ (%)	79.1 (50.4)
No. of amino-acid residues	160
No. of solvent molecules	26
R factor (%)	17.5 (24.8)
R_{free} (%)	23.6 (36.4)
R.m.s.d.§	
Bond length (Å)	0.0061
Bond angle (°)	1.2
Dihedrals (°)	25.0
Impropers (°)	0.68
Mean temperature factors ($Å^2$)	
Main chain	26.3
Side chain	28.5
Solvent	25.3
Mean atomic coordinate error¶ (Å)	0.26

† The volume per unit protein molecular weight (Matthews, 1968). ‡ $R_{merge} = \sum|I - \langle I\rangle|/\sum I$. § Root-mean-square-deviation. ¶ Obtained from a Luzzati plot (Luzzati, 1952).

2.3. Crystallization

Single crystals of hCyPJ were grown at 293 K using the macroseeding technique. The hCyPJ seeds were obtained by the hanging-drop vapour-diffusion method: protein at a concentration of 10 mg ml^{-1} was mixed in a 1:1 ratio with reservoir solution containing 0.1 *M* Tris–HCl pH 8.0, 17–20%(*w*/*v*) PEG 8000, 3% DMSO. Thin plate-shaped crystals grew within one week; these were cut into small pieces and used as seeds. Each seed was washed and then seeded into a fresh hanging drop pre-equilibrated over the reservoir solution. The composition of the reservoir solution for seeding was the same as mentioned above except that the concentration of PEG 8000 was reduced to 13–15%(*w*/*v*). This macroseeding procedure was repeated one or two times to give crystals with dimensions of approximately 0.4 × 0.3 × 0.1 mm, most of which were twinned crystals; however, one was a single crystal and was used to collect data set 1.

The seeding conditions were further improved by increasing the concentration of DMSO to 6% and changing the pH value of the reservoir solution to 7.6. A single crystal with dimensions of 0.3 × 0.3 × 0.1 mm grown under the improved conditions was used to collect data set 2.

2.4. X-ray data collection

Two sets of X-ray data were collected to 3.0 Å resolution for data set 1 and to 2.6 Å resolution for data set 2 using a laboratory X-ray source equipped with a CCD detector.

The X-ray data were processed using *HKL*2000 (Otwinowski & Minor, 1997). The crystals belong to the trigonal space group $P321$, $P3_121$ or $P3_221$, with unit-cell parameters $a = b = 41.3$, $c = 172.1$ Å. Whether there is a screw axis could not be identified at this stage as sufficient 00*l* reflections had not been collected. The crystal data and the data-collection statistics of data set 2 are shown in Table 1.

2.5. Structure determination and refinement

The three-dimensional structure of hCyPJ was determined by molecular replacement with the program *AMoRe* (Navaza, 1994) using the molecular structure of hCyPA at 1.63 Å resolution as the search model (PDB code 2cpl; Ke, 1992) in which the eight N-terminal residues were omitted and the residues that differed between the two protein sequences were all replaced by alanine. Molecular replacement was carried out with space groups $P321$, $P3_121$ and $P3_221$ in turn using data set 1 in the resolution range 10–4 Å. The translation function gave an unambiguous solution only with space group $P3_121$; no predominant peak was observed in the other two space groups. The space group was thus determined to be $P3_121$, with unit-cell parameters $a = b = 41.3$, $c = 172.1$ Å and one molecule per asymmetric unit. The solution from the rotation and translation functions ($\alpha = 114.49$, $\beta = 51.19$, $\gamma = 77.99^\circ$, $T_x = 0.5647$, $T_y = 0.2213$, $T_z = 0.0860$) was applied to the search model and rigid-body refinement was performed, giving an initial electron-density map and an R factor of 0.49 at 3 Å resolution. The initial hCyPJ structure model was then established based on the electron-density map and the true sequence of hCyPJ.

Crystallographic refinement was then carried out using *CNS* (Brünger *et al.*, 1998) and manual model refitting was performed using *TURBO-FRODO* (Roussel & Cambillau, 1991). The refinement was carried out using data sets 1 and 2 successively. Solvent molecules were added to the model at late stage of the refinement and only those with B values less than 50 Å^2 were included in the final model.

2.6. Quality of the structure

The hCyPJ structure was refined at 2.6 Å resolution. The R factor and $R_{\rm free}$ are 17.5 are 23.6%, respectively. The Ramachandran plot calculated using *PROCHECK* (Morris *et al.*, 1992) shows that 83.1, 16.2 and 0.7% of residues are in most favoured, additional allowed and generously allowed regions, respectively. The refinement statistics are shown in Table 1.

3. Results

3.1. Overall structure

Fig. 1 shows the sequence of hCyPJ aligned with hCyPA and other representative members of the CyP family for which three-dimensional structures have been reported. hCyPJ shows 50% identity to hCyPA and 45–51% identity to human CyPB, murine CyPC and human CyPH.

There is one hCyPJ molecule in each asymmetric unit, which contains 160 amino acids and 26 solvent molecules. The C-terminus, Gln161, displayed poor electron density and could not be located. There is one disulfide bridge in each hCyPJ molecule, formed by Cys18 and Cys25. The ribbon diagram of the hCyPJ structure is shown in Fig. 2.

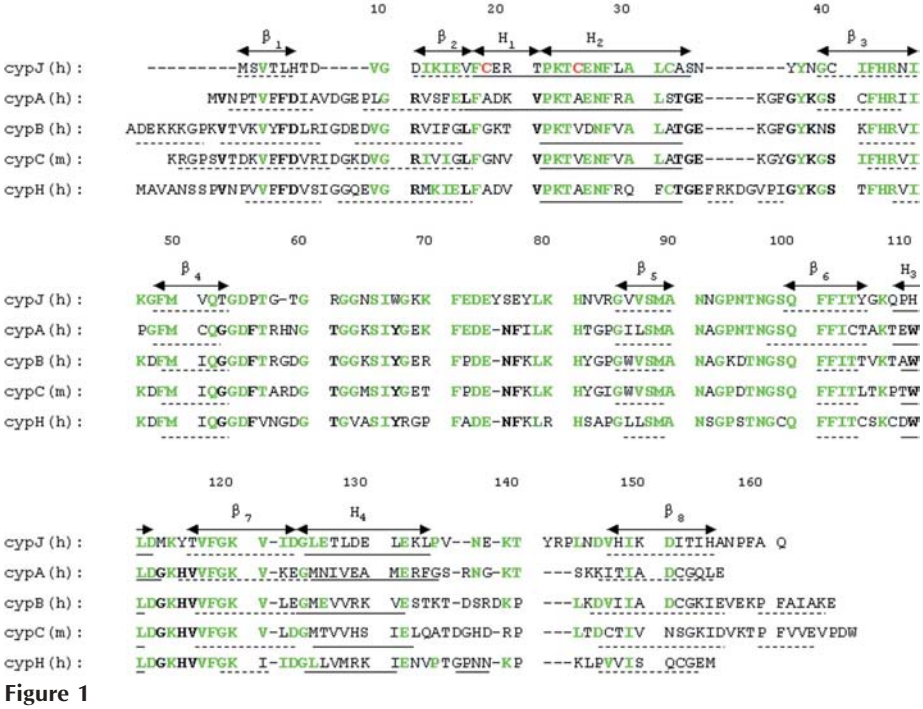

Figure 1
Sequence of hCyPJ aligned with those of the representative members of CyP family hCyPA, human CyPB, murine CyPC and human CyPH. The β-strands and helices of each protein are underlined with dotted lines and solid lines, respectively, and those of hCyPJ are also labelled as β and H, respectively. Cys18 and Cys25 forming a disulfide bridge are shown in red. Residues identical in hCyPJ and any other member are shown in green and residues which are identical in the other four members but different in hCyPJ are shown in black and bold.

3.2. Secondary structure

The secondary structure of hCyPJ is shown in Figs. 1 and 2 and is similar to those of other CyPs. Each hCyPJ molecule contains four helices and one β-barrel. The β-barrel is composed of eight antiparallel β-strands arranged clockwise in the order $\beta1$, $\beta2$, $\beta7$, $\beta5$, $\beta6$, $\beta4$, $\beta3$, $\beta8$ when the β-barrel is viewed from the top (Fig. 2). The segment Phe17–Thr21 forms a short helix, H1, with the carbonyl O atom of Phe17 being within hydrogen-bonding distance of the amide N atoms of both Arg20 and Thr21. H2 follows H1,

starting at Pro22. H2 and H4 are standard α-helices and are located at the bottom and the top of the β-barrel, respectively, and a short 3_{10}-helix, H3, is on one side of the barrel (Fig. 2).

3.3. Tertiary structure

The tertiary structure of hCyPJ is also similar to that of hCyPA. The r.m.s. deviation of the C^{α} atoms between the two structures is 1.8 Å. In addition to the shorter N-terminal segment and the longer C-terminal segment, obvious differences in the tertiary structure between the two proteins were observed in the segments Asp8–Val9, Cys32–Asn35, Asp73–Leu79 and Pro135–Asn145 of hCyPJ, as shown in Fig. 3. All these segments of hCyPJ contain deletions or insertions in the sequence (Fig. 1) and are located at the molecular surface. Asp8 and Val9 of hCyPJ directly connect with each other, whereas the two corresponding residues in hCyPA are linked by a loop owing to a five-residue deletion in hCyPJ. Each of the segments Cys32–Asn35 and Asp73–Leu79 of hCyPJ contains a β-turn: the former precedes a three-residue deletion and the latter contains an insertion compared with hCyPA. The segment Pro135–Asn145 forms a large loop containing three hydrogen bonds, Pro135 O···Leu144 N, Asn137 N···Arg142 O, Asn137 O···Tyr141 N, and the tertiary structure of hCyPJ shows the most striking differences in this segment from that of hCyPA, which is attributed to one deletion and a three-residue insertion in this segment. The biological implications of these differences are discussed below.

3.4. Active-site structure

It was reported that in the structure of hCyPA–CsA complex the water molecule Wat18 played a pivotal role and was within hydrogen-bonding distances of the two active-site residues His54 and Gln63 (Mikol *et al.*, 1993). These two residues correspond to His43 and Gln52 of hCyPJ based on the sequence alignment (Fig. 1). Therefore, His43 and Gln52 are expected to be the active sites of hCyPJ. A water molecule, Wat226, was found to be close to these two residues in the hCyPJ structure. Fig. 4(*a*) shows the electron density of His43, Gln52 and the nearby segment Thr59-Gly60-Arg61 of hCyPJ as well as Wat226. Fig. 4(*b*) shows these residues and Wat226 superimposed with the corresponding residues in the hCyPA–CsA complex structure.

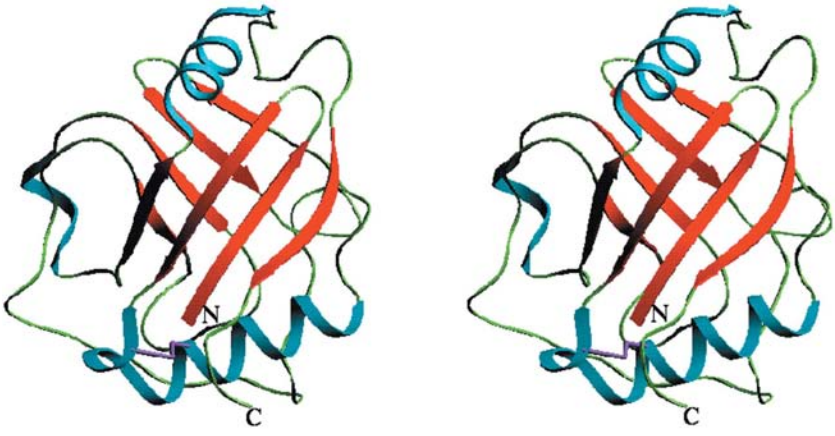

Figure 2
Ribbon diagram of hCyPJ. Helices, β-strands and random coils are shown in blue, red and green, respectively. The disulfide bridge is shown in violet. The N- and C-termini are labelled. This diagram was prepared using the program *SETOR* (Evans, 1993).

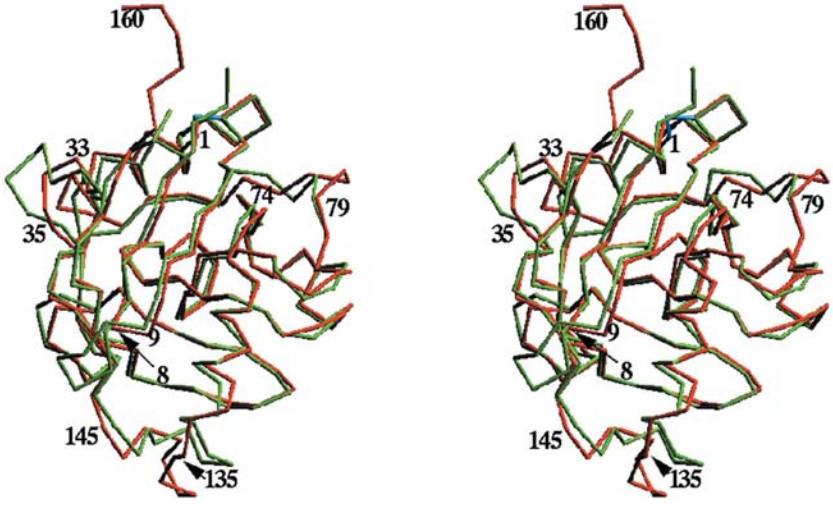

Figure 3
C^{α} backbone of hCyPJ superimposed with that of hCyPA. hCyPJ is shown in red and hCyPA in green. The residue numbers of Met1, Asp8, Val9, Ala33, Asn35, Glu74, Leu79, Pro135, Asn145 and Ala160 of hCyPJ are labelled. This diagram was prepared using the program *SETOR*.

4. Discussion

Various members of the CyP family exhibit sequence homology, as shown in Fig. 1. The secondary structures are also conserved in the CyP family, with an eight-stranded antiparallel β-barrel and several helices in each member of the family (Fig. 1). When the detailed secondary structures of hCyPJ and hCyPA are compared with each other, the entire H4 of hCyPJ is an α-helix while the corresponding helix of hCyPA consists of two portions: an α-helix in the N-terminal part and a 3_{10}-helix in the C-terminal part (Ke, 1992). β1 and β2 of hCyPJ are slightly shorter than those of hCyPA at the C-terminal part of β1 and the N-terminal part of β2 owing to a five-residue deletion between the two β-strands.

Cys18 and Cys25 form a disulfide bridge in hCyPJ (Figs. 1 and 2). These two cysteines are not conserved in other CyPs; for example, both are replaced by alanines in hCyPA. The other two cysteines, Cys32 and Cys40, of hCyPJ do not form a disulfide bridge. There are four cysteine residues in hCyPA and no disulfide bridge is formed between them (Ke, 1992); the corresponding residues in hCyPJ are not cysteines.

The tertiary structure of hCyPJ is similar to that of hCyPA, but the segments Asp8–Val9, Cys32–Asn35, Asp73–Leu79 and Pro135–Asn145 of hCyPJ exhibit striking differences from those of hCyPA, as described above. However, neither of these segments would be close to CsA and involved in interactions with it based on the hCyPA–CsA complex structure. Arg148 of hCyPA was reported to be an important contact site for calcineurin (Etzkorn *et al.*, 1994) and there is a deletion at the corresponding position in the sequence of hCyPJ. This deletion is located in the segment Pro135–Asn145 of hCyPJ, which shows large differences in sequence and structure from other CyPs (Figs. 1 and 3). This loop is likely to contribute to the functional specificity; for example, it probably modulates calcineurin inhibition, as suggested by the large structural differences in the corresponding loop between the hCyPA–CsA and CyPB–CsA complexes based on the fact that the CyPB–CsA complex is 14-fold more effective than the hCyPA–CsA complex in inhibiting calcineurin (Mikol *et al.*, 1994).

The structure of hCyPA complexed with CsA showed that the water molecule Wat18 played a pivotal role and was within hydrogen-bonding distance of His54 NE2 and Gln63 NE2 and that Wat19 was hydrogen bonded to Wat18 and to the carbonyl O atom of Asn71 (Mikol *et al.*, 1993). In the uncomplexed hCyPA structure (at 1.63 Å resolution) two water molecules, Wat201 and Wat208, correspond to Wat18 and Wat19 of the hCyPA–CsA complex (at 2.1 Å resolution), respectively, but they are moved by 0.5 and 1.0 Å, respectively, after binding CsA. The active-site residues His43 and Gln52 of hCyPJ superimpose quite well with His54 and Gln63 of hCyPA in the hCyPA–CsA complex, respectively, which is shown in Fig. 4(*b*). Wat226 in the hCyPJ structure is a conserved solvent molecule corresponding to Wat201 in the uncomplexed hCyPA and Wat18 in the hCyPA–CsA complex; however, it is approximately 0.9 Å from Wat18 of the hCypA–CsA complex when the two structures are superimposed (Fig. 4*b*) and it is 3.8 and 3.5 Å away from the NE2 atoms of His43 and Gln52, respectively, which are beyond hydrogen-bonding distance. Although the position of Wat226 may not be very accurate in the structure at 2.6 Å resolution, the movement of the corresponding water molecule in hCyPA, which was observed by comparing the unligated and complexed hCyPA structures, both at high resolution, suggests that Wat226 of hCyPJ is likely to be involved in catalysis by moving closer to His43 and Gln52 after binding substrate. The segment Thr59-Gly60-Arg61 of hCyPJ can be superimposed with Asn71-Gly72-Thr73 of hCyPA; however, in the hCyPJ

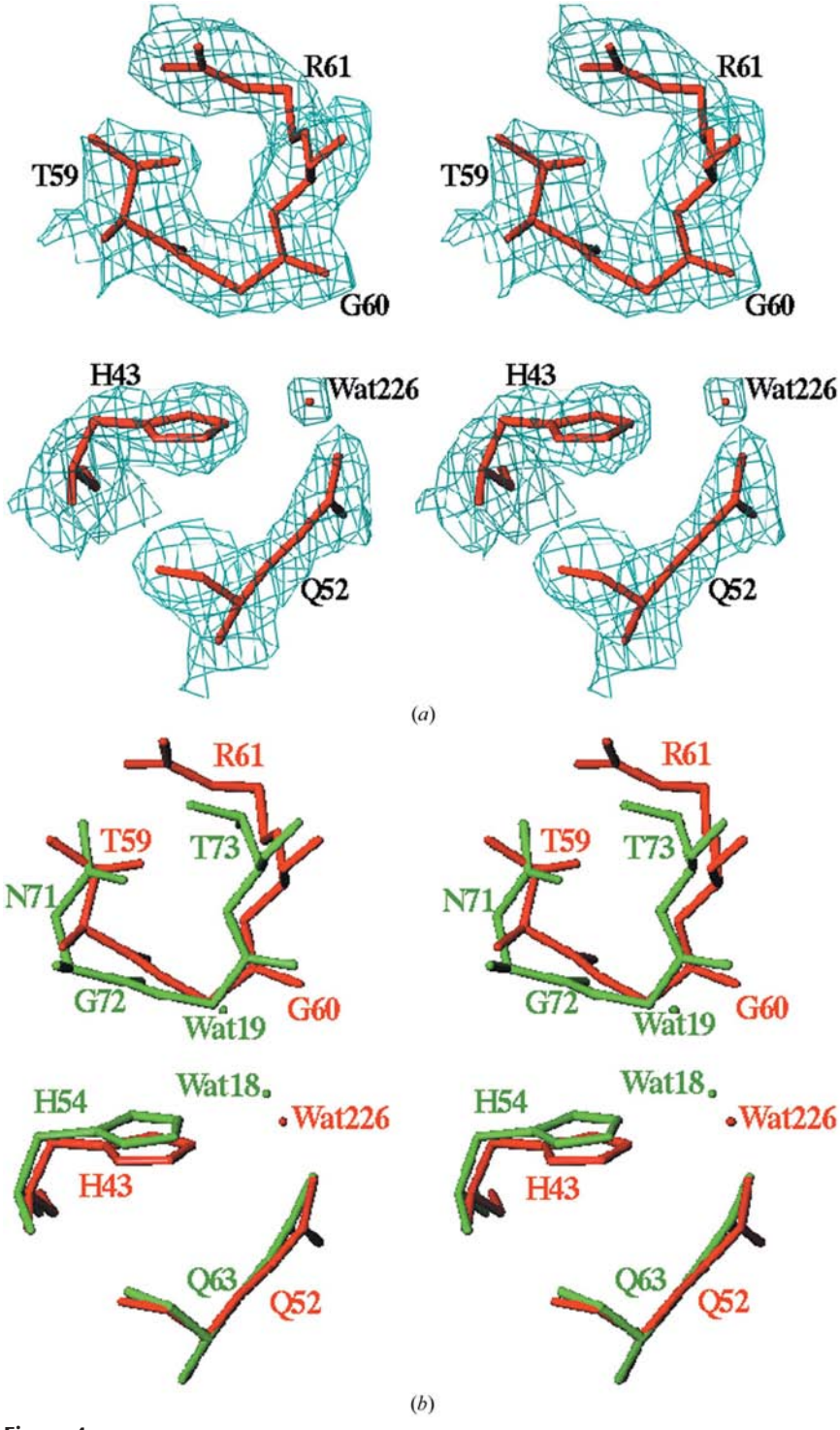

Figure 4
The active-site structure. (*a*) ($2F_o - F_c$) electron density contoured at 1.0σ of His43, Gln52 and the segment Thr59–Arg61 as well as Wat226. (*b*) These residues and the water molecule superimposed with the corresponding ones in the hCyPA–CsA complex structure. hCyPJ and hCyPA are shown in red and green, respectively. These diagrams were prepared using the program *TURBO-FRODO*.

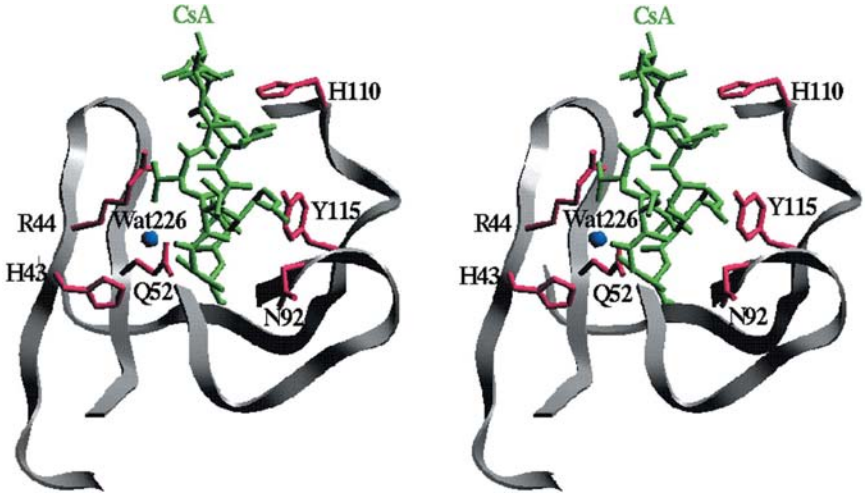

Figure 5
His43, Arg44, Gln52, Asn92, His110, Tyr115 and Wat226 of the hCyPJ structure. The side chains of the six residues are shown in red and Wat226 is shown in blue. The hCyPA–CsA structure was superimposed with hCyPJ and only CsA is shown in green.

structure no water molecule was found to correspond to Wat19 of the hCyPA–CsA complex, probably because of the lower resolution of the hCyPJ structure. Of the several different mechanisms proposed previously, each of which only explains part of the experimental data, a solvent-assisted mechanism for the *cis–trans* isomerization was proposed based on the observation that a water molecule consistently bound to the side chain of Gln63 in both structures of the unligated hCyPA and the hCyPA–dipeptide (Ala-Pro) complex. This water molecule was proposed to be a candidate to stabilize the transition state of the amide bond (Ke, Mayrose *et al.*, 1993; Zhao & Ke, 1996). The hCyPJ structure appears to support this mechanism since it shows the conserved water molecule.

As observed in the hCyPA–CsA complex structure, 13 residues of hCyPA define a hydrophobic binding pocket and are within 4.0 Å of the bound CsA (Mikol *et al.*, 1993). They correspond to Arg44, Phe49, Met50, Gln52, Gly60, Ala90, Asn91, Asn92, Gln100, Phe102, His110, Leu111 and Tyr115 of hCyPJ. All of these residues are conserved in primary sequence except for three residues: Asn92, His110 and Tyr115 of hCyPJ replace Ala103, Trp121 and His126 of hCyPA, respectively. The positions of His43, Gln52 and Wat226 are similar to the corresponding residues of hCyPA, as described above, and the conserved residue Arg44 nearby may also be important. They are located at one side of CsA when the CsA coordinates were taken from the superimposed hCyPA–CsA complex structure, as shown in Fig. 5. Asn92, His110 and Tyr115, which are not conserved in the sequence, are on the other side, which is also shown in Fig. 5. In the hCyPA–CsA complex structure the residue corresponding to Asn92 is an alanine and the side chain of Asn92 of hCyPJ might slightly change conformation to form an additional hydrogen bond to CsA. Trp121 of hCyPA forms a strong hydrogen bond to CsA and this hydrogen bond is expected to remain in hCyPJ since the imidazole of His110 of hCyPJ superimposes well with the five-membered ring of the tryptophan of hCyPA. The hydroxyl group of Tyr115 of hCyPJ might form a hydrogen bond to CsA and the change from His126 of hCyPA to the larger Tyr115 of hCyPJ might lead to conformational changes of either this side chain or CsA in order to avoid unreasonably close contacts. The crystal structure of hCyPJ suggests that hCyPJ binds CsA with similar active-site structure, but the binding details may be somewhat different from those in the hCyPA–CsA complex.

References

Brünger, A. T., Adams, P. D., Clore, G. M., DeLano, W. L., Gros, P., Gross-Kunstleve, R. W., Jiang, J.-S., Kuszewski, J., Nilges, N., Pannu, N. S., Read, R. J., Rice, L. M., Simonson, T. & Warren, G. L. (1998). *Acta Cryst.* D**54**, 905–921.

Etzkorn, F. A., Chang, Z., Stolz, L. A. & Walsh, C. T. (1994). *Biochemistry*, **33**, 2380–2388.

Evans, S. V. (1993). *J. Mol. Graph.* **11**, 134–138.

Gamble, T. R., Vajdos, F. F., Yoo, S., Worthylake, D. K., Houseweart, M., Sundquist, W. I. & Hill, C. P. (1996). *Cell*, **87**, 1285–1294.

Goethel, S. F. & Marahiel, M. A. (1999). *Cell. Mol. Life Sci.* **55**, 423–436.

Handschumacher, R. E., Harding, M. W., Rice, J., Drugge, R. & Speicher, D. W. (1984). *Science*, **226**, 544–547.

Howard, B. R., Vajdos, F. F., Li, S., Sundquist, W. I. & Hill, C. P. (2003). *Nature Struct. Biol.* **10**, 475–481.

Kallen, J., Spitzfaden, C., Zurini, M. G. M., Wider, G., Widmer, H., Wuthrich, K. & Walkinshaw, M. D. (1991). *Nature (London)*, **353**, 276–279.

Karmela, B. (1995). *Acta Pharm.* **45**, 413–420.

Ke, H. (1992). *J. Mol. Biol.* **228**, 539–550.

Ke, H., Mayrose, D. & Cao, W. (1993). *Proc. Natl Acad. Sci. USA*, **90**, 3324–3328.

Ke, H., Zhao, Y., Luo, F., Weissman, I. & Friedman, J. (1993). *Proc. Natl Acad. Sci. USA*, **90**, 11850–11854.

Ke, H., Zydowsky, L. D., Liu, J. & Walsh, C. T. (1991). *Proc. Natl Acad. Sci. USA*, **88**, 9483–9487.

Luzzati, P. V. (1952). *Acta Cryst.* **5**, 802–810.

Matthews, B. W. (1968). *J. Mol. Biol.* **33**, 491–497.

Mikol, V., Kallen, J., Pflugl, G. & Walkinshaw, M. D. (1993). *J. Mol. Biol.* **234**, 1119–1130.

Mikol, V., Kallen, J. & Walkinshaw, M. D. (1994). *Proc. Natl Acad. Sci. USA*, **91**, 5183–5186.

Morris, A. L., MacArthur, M. W., Hutchinson, E. G. & Thornton, J. M. (1992). *Proteins Struct. Funct. Genet.* **12**, 345–364.

Navaza, J. (1994). *Acta Cryst.* A**50**, 157–163.

Otwinowski, Z. & Minor, W. (1997). *Methods Enzymol.* **276**, 307–326.

Peterson, M. R., Hall, D. R., Berriman, M., Nunes, J. A., Leanard, G. A., Rairlamb, A. H. & Hunter, W. N. (2000). *J. Mol. Biol.* **298**, 123–133.

Reidt, U., Wahl, M. C., Fasshauer, D., Horowitz, D. S., Luhrmann, R. & Ficner, R. (2003). *J. Mol. Biol.* **331**, 45–56.

Roussel, A. & Cambillau, C. (1991). *Silicon Graphics Partners Geometry Directory.* Mountain View, CA, USA: Silicon Graphics.

Takahashi, N., Hayano, T. & Suzuki, M. (1989). *Nature (London)*, **337**, 473–478.

Zhao, Y., Chen, Y., Schutkowsky, M., Fischer, G. & Ke, H. (1997). *Structure*, **5**, 139–146.

Zhao, Y. & Ke, H. (1996). *Biochemistry*, **35**, 7362–7368.

Zhou, Z., Ying, K., Dai, J., Tang, R., Wang, W., Huang, Y., Zhao, W., Xie, Y. & Mao, Y. (2001). *Cytogenet. Cell Genet.* **92**, 231–236.